J Fluoresc (2015) 25:1897–1904
DOI 10.1007/s10895-015-1682-2

ORIGINAL ARTICLE

Binding of Metallated Porphyrin-Imidazophenazine Conjugate to Tetramolecular Quadruplex Formed by Poly(G): a Spectroscopic Investigation

Olga Ryazanova[1] · Victor Zozulya[1] · Igor Voloshin[1] · Larysa Dubey[2] · Igor Dubey[2] · Victor Karachevtsev[1]

Received: 9 July 2015 / Accepted: 28 September 2015 / Published online: 8 October 2015

Abstract The binding of telomerase inhibitor ZnTMPyP^{3+}–ImPzn, Zn(II) derivative of tricationic porphyrin–imidazophenazine conjugate, to tetramolecular quadruplex structure formed by poly(G) was studied in aqueous solutions at neutral pH and near physiological ionic strength using absorption and polarized fluorescent spectroscopy techniques. Three binding modes were determined from the dependences of the fluorescence intensity and polarization degree for the porphyrin and phenazine moieties of the conjugate on molar polymer-to-dye ratio (*P*/*D*). The first one is outside electrostatic binding of positively charged porphyrin fragments to anionic phosphate groups of the polymer which prevails only at very low *P*/*D* values and manifests itself by substantial fluorescence quenching. It is suggested that the formation of externally bound porphyrin dimers occurs. The other two binding modes observed at high *P*/*D* are embedding of the ZnTMPyP^{3+} moiety into the groove of poly(G) quadruplex accompanied by more than 3-fold enhancement of the conjugate emission, and simultaneous intercalation of the phenazine fragment between the guanine bases accompanied by the increase of its fluorescence polarization degree up to 0.25. Thus Zn(II) conjugate seems to be promising ligand for the stabilization of G-quadruplex structures since porphyrin binding to poly(G) is strengthened by additional intercalation of phenazine moiety.

Keywords Porphyrin–imidazophenazine conjugate · Poly(G) · G-quadruplex · Absorption · Fluorescence

Introduction

Specific four-stranded DNA and RNA structures known as G-quadruplexes (G4) are highly polymorphic arrangements formed by stacked arrays of guanine quartets connected by non-canonical Hoogsteen-type hydrogen bonds. They play a crucial biological role and are currently considered as promising targets for anticancer strategy. The sequences able to fold into G4 structures predominate in telomeric DNA, although they also have been found in a number of gene promoter regions, primarily in proto-oncogenes like *c-myc* or *k-ras* [1–3]. There are intra- and intermolecular quadruplexes, with parallel, antiparallel and hybrid-type topologies [2, 4–6]. For example, 22-mer oligonucleotide Tel22, a human telomeric DNA sequence, forms a parallel type intramolecular G-quadruplex in the presence of K^+ ions [7].

Polyguanylic acid, poly(G), as well as poly(dG), are known to form stable four-stranded telomere-like helical structure [8] with arrangements of G-tetrads stacked on one another [6, 9]. These polymers are suitable models of G-quadruplex regions of telomeric DNA to study ligand-quadruplex interactions.

The binding of a drug to telomeric quadruplexes may stabilize G4 structures and inhibit the telomerase enzyme expressed in most cancer cells (in contrast to normal somatic cells) that results in anticancer activity [1, 3, 4, 10, 11]. The structure of G-quadruplexes strongly differs from that of

✉ Olga Ryazanova
ryazanova@ilt.kharkov.ua

[1] Department of Molecular Biophysics, B. Verkin Institute for Low Temperature Physics and Engineering, National Academy of Sciences of Ukraine, 47 Lenin ave, 61103 Kharkov, Ukraine

[2] Department of Synthetic Bioregulators, Institute of Molecular Biology and Genetics, National Academy of Sciences of Ukraine, 150 Zabolotnogo str, 03680 Kyiv, Ukraine

single- and double-stranded nucleic acids allowing their specific recognition by small molecules. The square of G-quartet, a key element of any quadruplex and the main target of G4 ligands, is twice as large as the square of usual DNA base pairs. Therefore, the specific G4 binder should have aromatic or heteroaromatic system larger than that required for duplex DNA ligands, to ensure an efficient π-π-interaction with its molecular target [4, 11]. The majority of efficient G-quadruplex binding/stabilizing ligands with anticancer properties, such as acridines, anthraquinones, carbazoles, macrocyclic polyoxazoles, etc. [4, 10, 11], contains heteroaromatic systems of this type. Large square planar porphyrin molecules may be ideal G4 ligands since they perfectly overlap with G-quartets.

Porphyrins play an important role in numerous biological processes, including e.g., photosynthesis, oxygen transport and respiration [12, 13]. Water-soluble cationic *meso*-substituted porphyrin 5,10,15,20-tetra-(N-methyl-4-pyridyl)porphine (TMPyP4) and its derivatives efficiently bind to DNA [14, 15], and can be used as photonucleases [16] and agents for photodynamic therapy [13, 17, 18]. Complexes of TMPyP4 and other cationic porphyrins with Red-Ox-active transition metals (Mn^{3+}, Fe^{3+}, Cu^{2+}, etc.) are able to perform oxidative DNA cleavage [19]. At the same time, TMPyP4 and its analogues possessing extended heteroaromatic systems were found to be efficient telomerase inhibitors and antitumor agents targeting G-quadruplexes of telomeric DNA [4, 10, 11].

Porphyrin conjugation to some other molecules can enhance its binding to G-quadruplex structures that can result in the increase of antitumor activity. The attachment of other molecular fragments to classic TMPyP4 is difficult, so its tricationic analog, $TMPyP^{3+}$, was employed. It can be easily functionalized, e.g., by introducing the carboxyalkyl or aminoalkyl group at *meso*-position, and thus is suitable for conjugation reactions. $TMPyP^{3+}$ porphyrin and its metal complexes were attached to a variety of molecules, including oligonucleotides for site-specific DNA cleavage or modification [20–22], peptides [23], ligands to obtain efficient DNA photocleavage and cytotoxic agents, including acridine [24], anthraquinone [25], phenylpiperazine [26], β-carboline [27], EDTA [28], C_{60} fullerene for molecular photoelectrochemical devices [29], etc. In these cases $TMPyP^{3+}$ derivatives were directed against duplex or single-stranded DNA. At the same time, there are several reports concerning the cationic porphyrin conjugates designed for improving the binding affinity to G-quadruplex DNA and its stabilization. These compounds include e.g., aminoquinoline [30, 31], anthraquinone [32] and bis-aminopropylamine [30] conjugates of $TMPyP^{3+}$.

To obtain an efficient G4 binder, we have attached $TMPyP^{3+}$ to imidazophenazine dye (ImPzn) via carboxyalkyl linker (Fig. 1) [33]. Imidazophenazine is known as DNA intercalating agent [34, 35], and we supposed that the attached dye would improve the porphyrin binding to G4 structures by intercalation between guanine quartets. It was shown that both $TMPyP^{3+}$–ImPzn conjugate and its Zn(II) and Mn(III) complexes at low micromolar concentrations inhibit telomerase in TRAP assay and demonstrate antiproliferative activity in vitro [33, 36]. The binding of these conjugates to intramolecular antiparallel G-quadruplex formed by model 22-mer oligonucleotide 5′-d[AGGG(TTAGGG)$_3$]-3′, a fragment of human telomeric DNA (Tel22, PDB code 143D), was studied using spectroscopic techniques [37]. It was shown that metaloconjugates stabilize Tel22 quadruplex. Also, the binding of non- metallated $TMPyP^{3+}$-ImPzn conjugate to poly(G)-based intermolecular quadruplex [8] was investigated [38]. It was found that this conjugate folds into stable intramolecular heterodimer which at high *P*/*D* incorporates into poly(G) quadruplex groove. Thus it seems appropriate to study the binding of metallated conjugate to the same quadruplex, since Zn(II) and Mn(III) porphyrin complexes are known to contain axial water ligands [39] which can prevent the formation of heterodimers and thus potentially improve the conjugate-G4 binding efficiency.

The aim of present work is to study the binding of Zn(II)$TMPyP^{3+}$–ImPzn derivative to tetramolecular quadruplex formed by poly(G) polynucleotide, to compare it with the data obtained for non-metallated conjugate and to determine effect of Zn^{2+} ion coordinated in the center of the porphyrin moiety on the conjugate binding modes.

Materials and Methods

Chemicals

Zinc(II) metal complexes of $TMPyP^{3+}$–ImPzn conjugate (Fig. 1) were synthesized and purified by the procedures described in [33]. In brief, tris(4-pyridyl)phenylporphine containing a carboxybutyl function [40] was conjugated to N_1-aminoalkyl derivative of imidazo[4,5-b]phenazine in the presence of BOP-HOBT coupling reagent, followed by N-methylation of pyridine residues by methyl iodide. Porphyrin ring was then metalated by heating with zinc acetate in demethylformamide-collidine mixture [41]. Imidazo[4,5-b]phenazine dye and its aminoalkyl derivatives were obtained in accordance with methods reported in [42]. Poly(G) polynucleotide from Sigma Chem. Co. were used as received.

The 2 mM phosphate buffer (pH 6.9) containing 0.5 mM EDTA and 0.1 M NaCl, prepared from deionized water, was used as a solvent.

The concentration of the conjugate was determined gravimetrically. The polynucleotide concentration was determined spectrophotometrically in aqueous solution at room temperature using the extinction values of ε_{252}=9900 M^{-1} cm^{-1} for poly(G) and ε_{260}=7140 M^{-1} cm^{-1} for poly(A)·poly(U). The

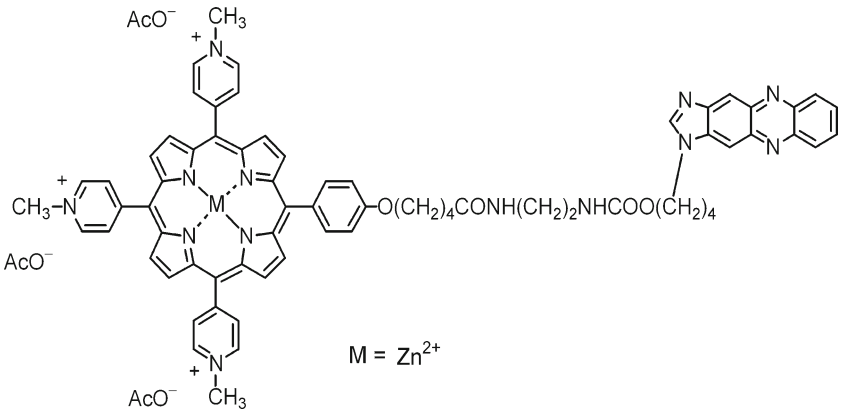

Fig. 1 Molecular structure of $ZnTMPyP^{3+}$–ImPzn conjugate

formation of four-stranded structure was proved by melting experiments with the registration of the temperature dependence of polymer absorbance at 295 nm in accordance with the procedure [43].

Apparatus and Techniques

The spectroscopic properties of metallated conjugate, $ZnTMPyP^{3+}$–ImPzn, in a free state (Fig. 1) and bound to four-stranded poly(G) have been studied using absorption and polarized fluorescent spectroscopy techniques.

Visible electronic absorption spectra were registered on SPECORD UV/VIS spectrophotometer (Carl Zeiss, Jena). Fluorescent measurements were carried out on laboratory spectrofluorimeter based on the DFS-12 monochromator (LOMO, 350–800 nm range, dispersion 5 Å/mm) by the method of photon counting [44]. The fluorescence was excited by the stabilized linearly polarized radiation of a halogen lamp in Soret band at λ_{ex}=440 nm. The emission was observed at an angle of 90° from the excitation beam. The fluorescence polarization degree, p, has been calculated from the equation:

$$p = \frac{I_{II} - I_{\perp}}{I_{II} + I_{\perp}} \quad (1)$$

where I_{II} and $I_{\perp}$ are intensities of the emitted light, which are polarized parallel and perpendicular to the polarization direction of exciting light, respectively. The spectroscopic experiments were carried out in quartz cells at room temperature from 20 to 22 °C.

To prove poly(G) four-stranded structure absorption melting of the polynucleotide at 295 nm was performed in the quartz cell allocated in the copper cell which temperature was changed by computer operated Peltier element. The thermal cell was inserted into the spectrophotometer.

To obtain the dependencies of the fluorescence intensity and polarization degree for porphyrin and phenazine moieties of the conjugate on P/D ratio, the series of fluorescence titration experiments were performed. Here the conjugate sample was added with increasing amounts of the concentrated poly(G) stock solution containing the same conjugate content of 10 μM to achieve the desired P/D value in the final solution, whereas fluorescence intensity and polarization degree were measured. The time from 7 to 10 min was required to reach the thermodynamic equilibrium in the system which was verified from the stability in the fluorescence signal.

Results

Absorption and Fluorescence Spectra of $ZnTMPyP^{3+}$–ImPzn

The visible absorption spectrum of free $Zn(II)TMPyP^{3+}$–ImPzn conjugate is presented in Fig. 2 along with spectra of its individual constituents, $Zn(II)TMPyP^{3+}$ and ImPzn [37]. It is seen that spectrum of the metallated porphyrin, $Zn(II)TMPyP^{3+}$, consists of the intense Soret band centered at 436 nm and two Q-bands at 564 and 610 nm. The visible spectrum of ImPzn is characterized by the absorption band at 385 nm and the longwave broad shoulder extending to 490 nm. The spectrum of the conjugate represents a superposition of the porphyrin and phenazine bands. Maximum of its Soret band is 9 nm red shifted in comparison with that for $Zn(II)TMPyP^{3+}$ (to 446 nm), and its extinction value is substantially less than in the parent porphyrin; Q-bands are red shifted to 572 and 621 nm correspondingly (Fig. 2).

Emission bands of the individual conjugate constituents are wide and structureless, their maxima lies at 658 nm for $Zn(II)TMPyP^{3+}$, and at 562 nm for ImPzn (Fig. 3). The shape of $ZnTMPyP^{3+}$–ImPzn spectrum is similar to that for parent Zn(II) porphyrin, but it is several times less intensive (Fig. 3), and the fluorescence band maximum is red shifted to 660 nm (Table 1). The fluorescence polarization degree is approximately 0.06 [37].

It can be noted that absorption bands of $ZnTMPyP^{3+}$–ImPzn are substantially red shifted in comparison with those for the non-metallated conjugate (for Soret band the shift value

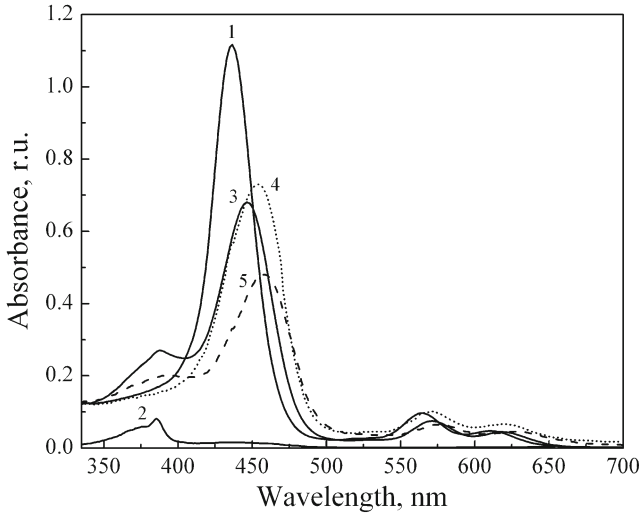

Fig. 2 Absorption spectra of individual ZnTMPyP^{3+} (1) and ImPzn (2) dyes, free ZnTMPyP^{3+}–ImPzn conjugate (3), ZnTMPyP^{3+} dye bound to poly(G) at P/D=107 (4) and ZnTMPyP^{3+}–ImPzn conjugate bound to poly(G) at P/D=49 (5) measured in aqueous buffered solution containing 0.1 M NaCl. Ligand concentration is 10 μM, path length is 0.5 cm

is 11 nm), that is typical for metallated porphyrin derivatives [39]. At the same time, maximum of ZnTMPyP^{3+}–ImPzn emission band is blue shifted in comparison with that for TMPyP^{3+}–ImPzn one [37]. The shape of emission bands is substantially different for these two compounds: spectrum of non-metallated conjugate consist of two distinct bands whereas the fluorescence band of Zn(II) conjugate remains unsplitted.

Absorption and fluorescence spectra of metallated and non-metallated conjugates were compared with those for parent compounds [33, 37, 45], and the differences were analyzed. It

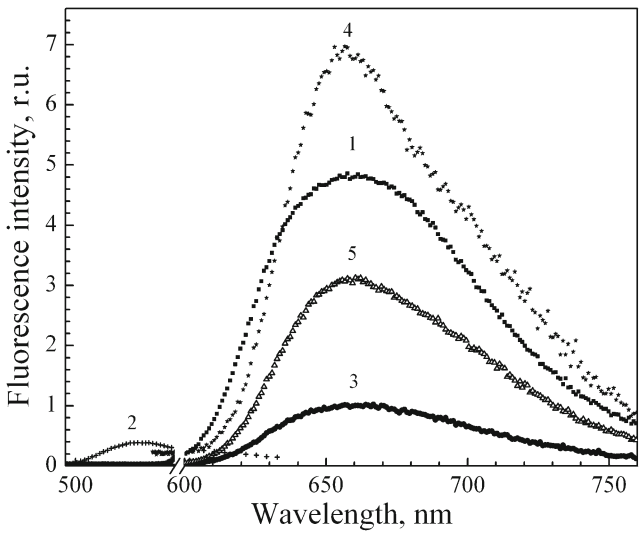

Fig. 3 Normalized fluorescence spectra of ZnTMPyP^{3+} (1) and ImPzn (2) dyes, ZnTMPyP^{3+}–ImPzn conjugate (3) in a free state, and of their complexes with the biopolymer at P/D=100: ZnTMPyP^{3+} + poly(G) (4), ZnTMPyP^{3+}–ImPzn+poly(G) (5), λ_{exc}=440 nm

was suggested that unlike to non-metallated TMPyP^{3+}–ImPzn conjugate which in the absence of the polymer folds into stable intramolecular heterodimer with π-π stacking between porphyrin and phenazine parts, for ZnTMPyP^{3+}–ImPzn, a heterodimer formation is presumably occurred too, but without a perfect stacking between the conjugate moieties due to sterical hindrances conditioned by Zn(II) axial ligand (coordination number of Zn^{2+}, n, is 5 or 6 for various compounds, for derivatives of TMPyP4 porphyrin n=5 was reported [39]). Possible structure of the heterodimer formed by ZnTMPyP^{3+}–ImPzn was calculated earlier using DFT method together with total and free Gibbs energy of their formation [33].

Fluorescent Titration Data

Binding of the Zn(II) conjugate to long four-stranded polyanionic chain of poly(G) polynucleotide was monitored in fluorescence titration experiment where changes in the relative fluorescence intensity and polarization degree on P/D ratio were registered near the emission band maxima of both porphyrin and phenazine moieties (Fig. 4), at λ_{obs}=655 and 547 nm correspondingly. Fluorescence was excited at 440 nm (in Soret band).

From Fig. 4 it is seen that titration curve registering the conjugate fluorescence intensity at 655 nm is biphasic. In the range of P/D from 0 to 1 addition of the polymer results in the essential fluorescence quenching up to 35 % from the initial value, as well as in the rise of fluorescence polarization degree. Further polymer addition (P/D>1) promotes monotonic increase in the conjugate emission, which then at P/D=9 returns to the initial level, and at P/D=100 becomes about 3 times more intensive than in the case of the free metallated conjugate (P/D=0). Fluorescence polarization degree also increases and reaches the steady level of 0.12 at these high P/D values.

Titration curves registered at 547 nm don't show any significant changes in the conjugate fluorescence intensity at this wavelength during the polymer addition, whereas fluorescence polarization degree increases monotonically up to higher steady level of 0.25.

Absorption and Fluorescence Spectra of Zn(II) Conjugate-Poly(G) Complex

The absorption and fluorescence spectra were obtained for complex of ZnTMPyP^{3+}–ImPzn and parent porphyrin with poly(G) at high polymer content (Figs. 2, 3). It was revealed that binding of the metallated conjugate to quadruplex poly(G) results in 9 nm red shift and 30 % hypochromism of its absorption spectrum (Fig. 2), as well as in substantial rise of the emission intensity (approximately 3.1-fold increase at P/D=100, see Fig. 3). The shape and position of the fluorescence band remains without any visible changes.

Table 1 Spectral characteristics of individual porphyrin and imidazophenazine dyes, the porphyrin–phenazine conjugates in a free state and bound to biopolymers measured in neutral aqueous buffered solution containing 0.1 M NaCl, λ_{exc}=440 nm

Compound	Absorption band maxima (nm)[a]	Fluorescence band maxima (nm)	Normalized fluorescence intensity, I/I_0		Fluorescence polarization degree, p	
$ZnTMPyP^{3+}$	436 564 610	658	–		0.013	
$TMPyP^{3+}$ [48]	385 425.5 522 561 583.5 642.5	717	–		0.015	
ImPzn [45]	385	562	–		0.015	
			at 655 nm	at 547 nm	at 655 nm	at 547 nm
$ZnTMPyP^{3+}$–ImPzn	388 446 572 621	660	1	1	0.06	0.15
$ZnTMPyP^{3+}$ –ImPzn+poly(G) (P/D=100)	454	660	3.1	0.96	0.12	0.25
$ZnTMPyP^{3+}$– ImPzn+poly(A)·poly(U) (P/D=120)	–	655	1.8	3.6	0.10	0.21
$ZnTMPyP^{3+}$ + poly(G) (P/D=100)	453	657	–	–	–	–
			at 670 nm	at 562 nm	at 670 nm	at 562 nm
$TMPyP^{3+}$–ImPzn [38]	435	673, 729	1	1	0.01	0.01
$TMPyP^{3+}$–ImPzn+poly(G) (P/D=115) [38]	446	678, 738	1.3	2.35	0.1	0.05
$TMPyP^{3+}$ [48]	425.5	717	1	–	0.015	–
$TMPyP^{3+}$ + poly(G) (P/D=115) [38]	446	679, 738	3.7	–	0.095	–
			at 700 nm	–	at 700 nm	–
$TMPyP^{3+}$ [48]	425.5	717	1	–	0.015	–
$TMPyP^{3+}$ + poly(P) (P/D=3.5) [48]	443	670, 725	0.2	–	0.060	–
$TMPyP^{3+}$ + poly(P) (P/D=115) [48]	426	661, 722	0.34	–	0.065	–

[a] For the porphyrins, conjugates and their complexes with polymers only position of Soret band maximum is presented

Spectroscopic properties of individual Zn^{2+} porphyrin and phenazin dyes, free $ZnTMPyP^{3+}$–ImPzn conjugate as well as their complex with poly(G) are summarized in Table 1.

Discussion

The shape of fluorescence titration curves as well as transformations of the conjugate spectra induced by the polymer addition indicates that both porphyrin and phenazine moieties of $ZnTMPyP^{3+}$–ImPzn bind to poly(G).

Initial part of the titration curve showing the changes in the fluorescence intensity of the porphyrin moiety (observation at 655 nm) somewhat differs from those observed earlier for binding of non-metallated conjugate and free porhyrins to oppositely charged polymers [38]. It is seen that the small initial polymer addition results in the 65 % fluorescence quenching. However we have not observed long linear descending part of the titration curve which is distinctive for binding of cationic dyes to polyanions, indicates the formation of the dye stacking aggregates on the charged polymer [46, 47] and gives a stoihiometric ratio of the binding. Least emission level for Zn(II) conjugate is higher than that for non-metallated one (35 and 20 % from initial value, correspondingly), and it corresponds to lower P/D values (for $TMPyP^{3+}$–ImPzn the curve minimum was at P/D=6). After P/D>1 the fluorescence intensity starts to increase, that evidences predomination of another binding mode. It is known that emission of tricationic $TMPyP^{3+}$ porphyrin dimers externally bound to single strand of inorganic polyphosphate, poly(P), has emission quenched up to 0.34 from initial (Table 1) [48] (this type of binding was observed at high P/D). Since for Zn

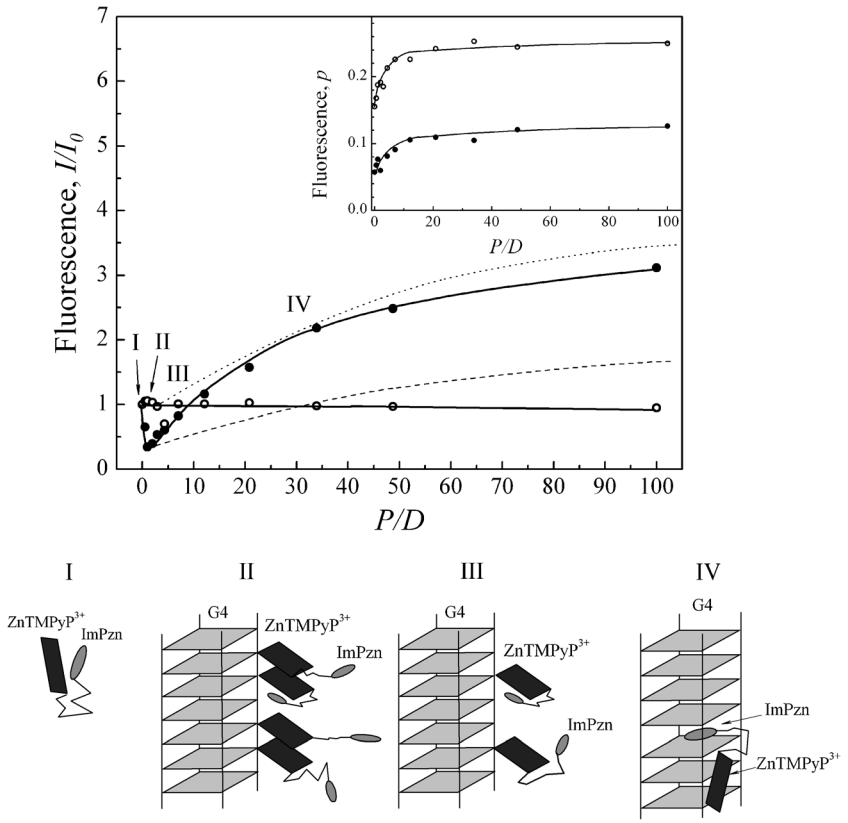

Fig. 4 Dependence of normalized fluorescence intensity and polarization degree (on the inset) on molar *P*/*D* ratio registered for $ZnTMPyP^{3+}$–ImPzn + poly(G) complex at λ_{obs}=655 (●) and 547 nm (○), as well as for $ZnTMPyP^{3+}$–ImPzn + poly(A)·poly(U) complex near the maximum of $TMPyP^{3+}$ emission band (dashed line) and ImPzn one (dotted line), λ_{exc}=440 nm. Pictorial diagram shows structure of complexes of $ZnTMPyP^{3+}$–ImPzn conjugate with tetramolecular poly(G) quadruplex presumably formed at different *P*/*D* ratios: (I) formation of internal heterodimers without perfect stacking in absence of the polymer (*P*/*D*=0); (II) disintegration of the heterodimers and outside binding of the porphyrin moieties of the conjugate to anionic poly(G) backbone with their pairwise self-stacking; (III) disintegration of stacked dimers and redistribution of bound conjugate molecules along the polymer, (IV) incorporation of $ZnTMPyP^{3+}$ moieties into poly(G) groove and intercalation of ImPzn moieties between guanine tetrads

conjugate bound to poly(G) minimal I/I_o=0.35 was registered at *P*/*D*=1, we can conclude that Coulomb interaction prevails only at very low *P*/*D* values: positively charged methylpyridil groups of the porphyrin bind to negatively charged phosphate groups of poly(G), but formation of long π-stacks does not occurs due to steric hindrance induces by zinc axial ligand. It is known that in different compounds Zn^{2+} ions have coordination number 5 or 6, thus, maximum two neighboring porphyrins can be stacked (see pictorial diagram in Fig. 4).

The further polymer addition induces substantial enhancement of the Zn(II) conjugate emission at 655 nm (porphyrin moiety) reaching I/I_o=3.1 at *P*/*D*=100, and the rise of fluorescence polarization degree up to 0.12 (Fig. 4). The fluorescence titration curve is steeper than for non-metalize conjugate, where only I/I_o=1.3 was reached at *P*/*D*=100 [38], and it is similar to that for the complex of individual $TMPyP^{3+}$ dye with poly(G) where I/I_o=3.7 at the same *P*/*D* value (Fig. 5). At the same time in all *P*/*D* range we have observed practically constant level of conjugate fluorescence at 547 nm (maximum of ImPzn emission) that can be explained by practically equal impacts of two effects: (i) quenching of ImPzn fluorescence upon the dye conjugation due to energy transfer from phenazine to porphyrin moiety registered for free conjugate and its complex with poly(G) at low *P*/*D*, as well as (ii) its quenching upon close contact with guanine residues when dye embeds into poly(G) due to photoinduced electron transfer between phenazine in the first singlet excited state and guanine in the ground state (at high *P*/*D*) [49]. To verify this hypothesis fluorescence titration curves were obtained for complex of the same metallated conjugate with double-stranded poly(A)·poly(U) polynucleotide (Fig. 4) which, as it is known, does not quench ImPzn fluorescence [49]. It was revealed that the fluorescence of ImPzn moiety remains unchanged in the initial part of fluorescent titration curve (*P*/*D*=0÷5), but further polymer addition results in the enhancement of the phenazine emission, so that at *P*/*D*=120 its fluorescence became 3.6 times more intensive than initial (*p*=0.21, see Table 1). As for the Zn $TMPyP^{3+}$ moiety of the conjugate, its emission quenches at the first poly(A)·poly(U) addition to 0.34 from initial, and it remains on this level in the *P*/*D* range from

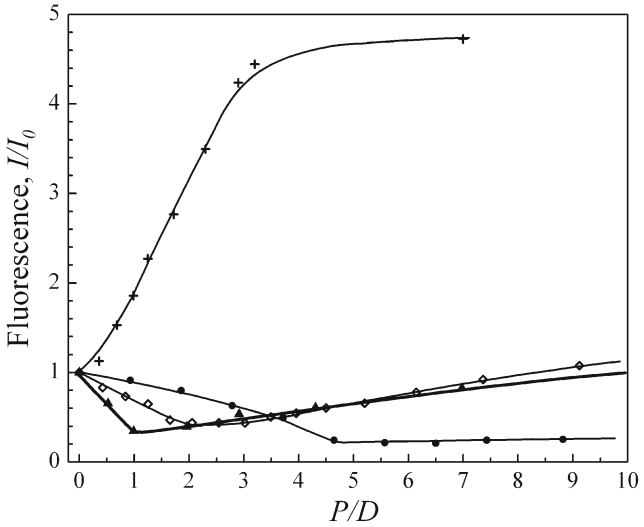

Fig. 5 Comparison of fluorescent titration curves (initial region) obtained as dependence of normalized porphyrin emission intensity on *P*/*D* ratio for tricationic porphyrin and porphyrin-phenazine conjugate bound to long quadruplexes formed by poly(G) and compact one formed by Tel22 oligonucleotide: ZnTMPyP^{3+}–ImPzn + poly(G) (▲), TMPyP^{3+}–ImPzn + poly(G) (●), ZnTMPyP^{3+}–ImPzn + Tel22 (✚) [37], TMPyP^{3+} + poly(G) (◇). Ligand concentration is 10 μM, λ_{exc}=440 nm, λ_{obs}=655 and 670 nm

0.38 to 4. Thus fluorescent characteristics of external binding mode are the same in the case of the Zn^{2+} conjugate bound to double stranded and quadruplex polymer. Further addition of the poly(A)·poly(U) results in the increase of the conjugate emission at 655 nm but the titration curve is less steep than in the case of poly(G), at *P*/*D*=120 only I/I_o=1.8 (p=0.1, see Table 1) was registered for complex of Zn(II)TMPyP^{3+}–ImPzn with poly(A)·poly(U) (for its complex with poly(G) this value was equal to 3.1). Enhancement of the porphyrin emission under its binding to poly(G) at high polymer content was observed also for non-metallated TMPyP^{3+} (Table 1, unpublished data), and earlier for Pheophorbide-*a* derivatives [50, 51].

Spectral transformation accompanying the binding of metallated conjugate to poly(G) at high *P*/*D* values were compared with those described by Fiel et al. in [52] for different types of TMPyP4 porphyrin binding to DNA, and data of Zozulya et al. [49] relating to binding of ImPzn to DNA and homopolynucleotides of various base composition. It allows us to suggest how the conjugate binds to the polymer. It is supposed that at high *P*/*D* values the porphyrin moiety embeds into the groove of the quadruplex chain that results in the red shift and hypochromism of absorption spectrum as well as in rise of the porphyrin emission. At the same time, the phenazine part intercalates between poly(G) nucleic bases, that is evidenced by substantial rise of fluorescence polarization degree (up to 0.25) obtained for this moiety (see pictorial diagram in Fig. 4). This assumption agrees well with data of Kelly and Murphy [53] showing that ZnTMPyP4 does not intercalate into DNA, as well as with the results obtained by Monaselidze et al. [54], revealing that metallization of the similar porphyrin by Zn^{2+} ions changes the mode of its binding to DNA from intercalation to groove binding. In our case, metallization of porphyrin part of conjugate also leads to a change in the type of the conjugate binding to four-stranded poly(G) as compared with data described in Ref. [38] for non-metallated one.

The fluorescent titration curves and spectra obtained for ZnTMPyP^{3+}–ImPzn bound to poly(G) were also compared with our data obtained earlier [37] for the same conjugate interacting with short 5′-d[AGGG(TTAGGG)$_3$]-3′ oligomer of human telomeric repeat (Tel22) under the same experimental conditions. It is known that at similar ionic conditions Tel22 forms intramolecular quadruplex containing only 3 guanine tetrads [5]. We have shown (Fig. 5) that in the case of ZnTMPyP^{3+}–ImPzn binding to Tel22 monotonically increasing titration curve without minimum have been registered, whereas with poly(G) the minimum near *P*/*D*=1 was observed where the emission was quenched up to 35 % from initial. So the quadruplex structure and the length of the polymer may play an important role in the type of complex formed.

Conclusions

Binding of the ZnTMPyP^{3+}–ImPzn conjugate to four-stranded poly(G) polynucleotide was investigated in neutral aqueous solution with near physiological content of Na^+ ions using various spectroscopic techniques. Results were compared with those obtained earlier for the interaction of non-metallated conjugate with the same polymer [38].

Unlike non-metallated TMPyP^{3+}–ImPzn which in the absence of the polymer folds into stable intramolecular heterodimer with π-π stacking between porphyrin and phenazine parts, for metallated ZnTMPyP^{3+}–ImPzn, a heterodimer formation occurs too, but without a perfect stacking between the chromophores, perhaps due to the presence of axial ligand on the metal ion.

It was found that both parts of metallated conjugate bind to intermolecular G-quadruplex formed by poly(G), and three binding modes were identified. Two of them relate to metalloporphyrin moiety and are competitive. The first one is accompanied by quenching of the porphyrin fluorescence and prevails at very low *P*/*D* values. It was determined as outside electrostatic binding of positively charged methylpyridyl groups of the porphyrin to polyanionic chain of nucleic acid. It is presumably realized in dimeric form with π-stacking between neighboring porphyrin chromophores, whereas phenazine parts are away from the polymer. We assumed that long porphyrin stacks are not formed on the polymer chain due to sterical hindrance induced by Zn(II) axial ligand. The second binding type prevails at high *P*/*D* values. It suggests that embedding of the separate ZnTMPyP^{3+} moieties of the conjugate into the groove of quadruple poly(G) occurs resulting in more

than 3-fold enhancement of the emission, which can be explained by chromophore dehydratation. The third binding mode relates to ImPzn moiety of the conjugate. It is supposed that phenazine fragments intercalate into the poly(G) quadruplex that is confirmed by the high value of the dye fluorescence polarization degree, which increases up to 0.25.

In such a way, Zn(II)-conjugate is more promising G-quadruplex stabilizing ligand as compared to non-metallated analogue, since additional intercalative binding of phenazine fragment enhances the binding of porphyrin fragment to G4. In contrast, this type of binding was not revealed for non-metallated conjugate which embeds into poly(G) groove as internal heterodimer. This suggestion is in perfect agreement with our recent experimental data on biological activity of the conjugates. Zn(II) complex was found to be several times more efficient telomerase inhibitor [36] and antiproliferative agent [33, 36] than non-metallated hybrid.

Compliance with Ethical Standards The authors declare that our manuscript complies with the all Ethical Rules applicable for this journal and that there are no conflicts of interests.

References

1. Balasubramanian S, Neidle S (2009) Curr Opin Chem Biol 13(3): 345–353
2. Collie GW, Parkinson GN (2011) Chem Soc Rev 40(12):5867–5892
3. Duchler M (2012) J Drug Target 20(5):389–400
4. Xu Y (2011) Chem Soc Rev 40(5):2719–2740
5. Dai J, Carver M, Yang D (2008) Biochimie 90(8):1172–1183
6. Burge S, Parkinson GN, Hazel P, Todd AK, Neidle S (2006) Nucleic Acids Res 34(19):5402–5415
7. Parkinson GN, Lee MP, Neidle S (2002) Nature 417:876–880
8. Pochon F, Michelson AM (1965) Proc Natl Acad Sci U S A 53: 1425–1430
9. Howard FB, Frazier J, Miles HT (1977) Biopolymers 16(4):791–809
10. De Cian A, Lacroix L, Douarre C, Temime-Smaali N, Trentesaux C, Riou J-F, Mergny J-L (2008) Biochimie 90(1):131–155
11. Monchaud D, Teulade-Fichou M-P (2008) Org Biomol Chem 6(4): 627–636
12. Dolphin D (ed) (1978) The porphyrins. Academic Press, New York
13. Josefsen LB, Boyle RW (2012) Theranostics 2(9):916–966
14. Munson BR, Fiel RJ (1992) Nucleic Acids Res 20(6):1315–1319
15. Sehlstedt U, Kim SK, Carter P, Goodisman J, Vollano JF, Norden B, Dabrowiak JC (1994) Biochemistry 33(2):417–426
16. Da Ros T, Spalluto G, Boutorine AS, Bensasson RV, Prato M (2001) Curr Pharm Des 7(17):1781–1821
17. O'Connor AE, Gallagher WM, Byrne AT (2009) Photochem Photobiol 85(5):1053–1074
18. Ormond AB, Freeman HS (2013) Materials 6(3):817–840
19. Pitié M, Boldron C, Pratviel G (2006) Adv Inorg Chem 58:77–130
20. Mestre B, Pratviel G, Meunier B (1995) Bioconjug Chem 6(4): 466–472
21. Li H, Fedorova OS, Trumble RW, Flechter TR (1997) Bioconjug Chem 8(1):49–56
22. Dubey I, Pratviel G, Meunier B (2000) J Chem Soc Perkin Trans 1: 3088–3095
23. Mezo G, Herenyi L, Habdas J, Majer Z, Mysliwa-Kurdziel B, Toth K, Csik G (2011) Biophys Chem 155(1):36–44
24. Ishikawa Y, Yamashita A, Uno T (2001) Chem Pharm Bull 49(3): 287–293
25. Zhao P, Hu L-C, Huang J-W, Zheng K-C, Liu J, Yu H-C, Ji L-N (2008) Biophys Chem 134(1–2):72–83
26. Jia T, Jiang Z-X, Wang K, Li Z-Y (2006) Biophys Chem 119(3): 295–302
27. Kumar D, Mishra BA, Shekar KPC, Kumar A, Akamatsu K, Kusaka E, Ito T (2013) Chem Commun 49(7):683–685
28. Schwach G, Thamyongkit P, Reith LM, Svejda B, Knor G, Pfragner R, Schoefberger W (2012) Bioorg Chem 40:108–113
29. Marczak R, Sgobba V, Kutner W, Gadde S, D'Souza F, Guldi DM (2007) Langmuir 23(4):1917–1923
30. Dixon IM, Lopez F, Esteve J-P, Tejera AM, Blasco MA, Pratviel G, Meunier B (2005) ChemBioChem 6(1):123–132
31. Maraval A, Franco S, Vialas C, Pratviel G, Blasco MA, Meunier B (2003) Org Biomol Chem 1(6):921–927
32. Zhao P, Hu L-C, Huang J-W, Fu D, Yu H-C, Ji L-N (2009) Dyes Pigm 83(1):81–87
33. Dubey LV, Ilchenko MM, Zozulya VN, Ryazanova OA, Pogrebnoy PV, Dubey IY (2011) Int Rev Biophys Chem 2(4):147–152
34. Zozulya V, Yu B, Dubey I, Fedoryak D, Makitruk V, Ryazanova O, Shcherbakova A (2003) Biopolym (Biospectrosc) 72(4):264–273
35. Ryazanova O, Dubey L, Dubey I, Zozulya V (2012) J Fluoresc 22(6):1431–1439
36. Negrutska VV, Dubey LV, Ilchenko MM, Dubey IY (2013) Biopolym Cell 29(3):169–176
37. Zozulya VN, Ryazanova OA, Voloshin IM, Dubey LV, Dubey IY (2011) Int Rev Biophys Chem 2(4):112–119
38. Ryazanova O, Zozulya V, Voloshin I, Dubey L, Dubey I, Karachevtsev V (2015) J Fluoresc 25:1013–1021
39. Pasternack RF, Gibbs EJ, Villafranca JJ (1983) Biochemistry 22(10):2406–2414
40. Casas C, Saint-Jalmes B, Loup C, Lacey CJ, Meunier B (1993) J Org Chem 58:2913–2917
41. Dubey I, Pratviel G, Meunier B (1998) Compt Rend Acad Sci (Paris), Ser IIC 1(4):259–267
42. Dubey L, Ryazanova O, Zozulya V, Fedoryak D, Dubey I (2011) Nucleosides Nucleotides Nucleic Acids 30(7–8):585–596
43. Mergny J-L, Phan A, Lacroix L (1998) FEBS Lett 435:74–78
44. Zozulya VN, Ryazanova OA, Voloshin IM, Glamazda AY, Karachevtsev VA (2010) J Fluoresc 20(3):695–702
45. Ryazanova OA, Voloshin IM, Makitruk VL, Zozulya VN, Karachevtsev VA (2007) Spectrochimica Acta - Part A: Mol Biomol Spectroscopy 66(4–5):849–859
46. Schwarz G, Klose S, Balthasar W (1970) Eur J Biochem 12(3): 454–460
47. Schwarz G, Klose S, Balthasar W (1970) Eur J Biochem 12(3): 461–467
48. Zozulya VN, Ryazanova OA, Voloshin IM, Ilchenko MM, Dubey IY, Glamazda AY, Karachevtsev VA (2014) Biophys Chem 185(1): 39–46
49. Zozulya V, Yu B, Löber G, Voloshin I, Winter S, Makitruk V, Shalamay A (1997) Biophys Chem 65(1):55–63
50. Ryazanova OA, Voloshin IM, Dubey IY, Dubey LV, Zozulya VN (2008) Ann N Y Acad Sci 1130:293–299
51. Ryazanova OA, Voloshin IM, Dubey IY, Dubey LV, Zozulya VN (2008) IFMBE Proc 20:397–400
52. Fiel R (1989) J Biomol Struct Dyn 6:1259–1274
53. Kelly JM, Murphy MJ, McConnell DJ, OhUigin C (1985) Nucleic Acids Res 13(1):167–184
54. Monaselidze J, Gorgoshidze M, Khachidze D, Kiladze M, Bregadze V, Kiziria E, Margaryan H, Hakobyan N (2013) Am J Anal Chem 4:744–748